Supplementary Material

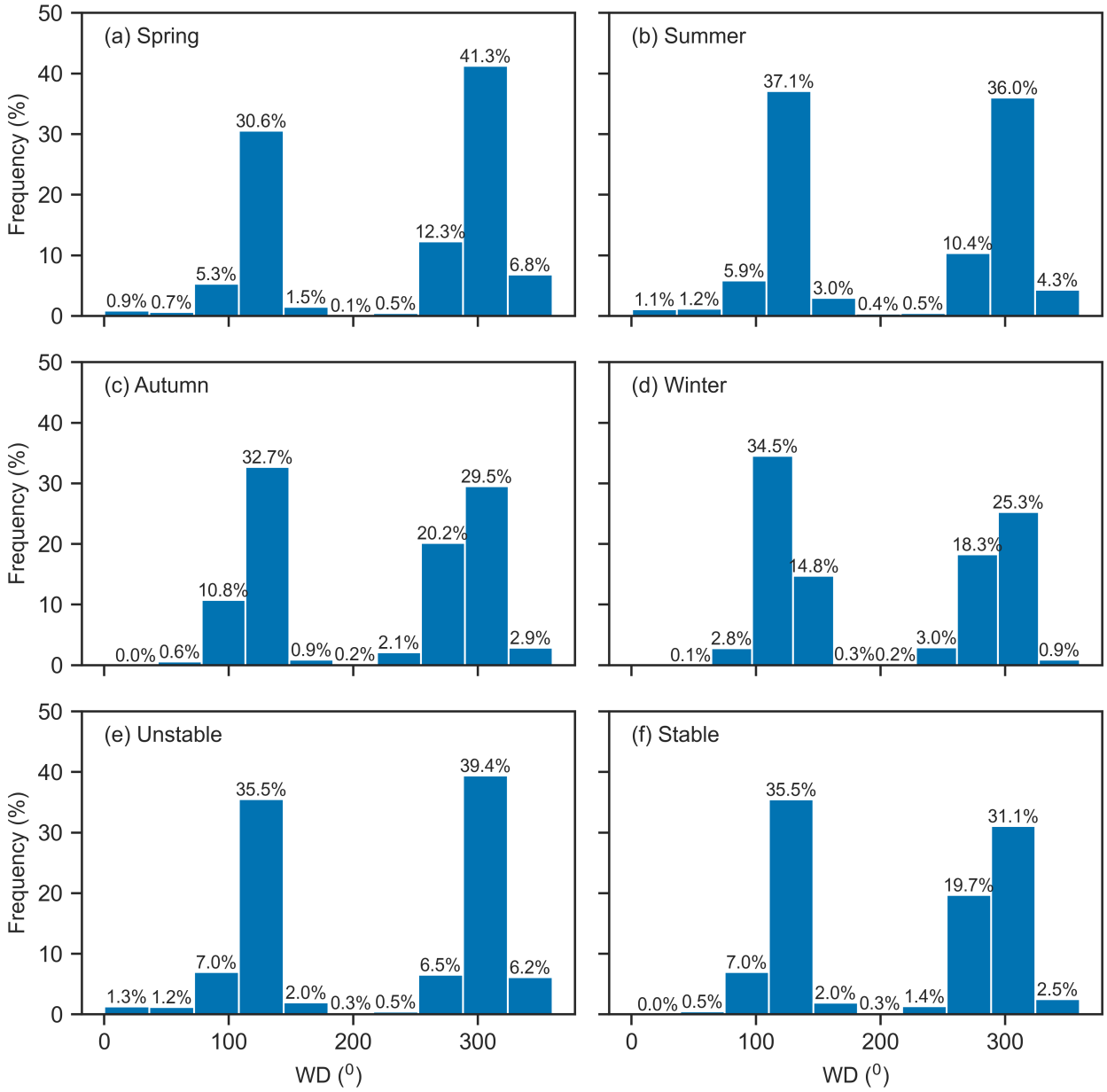

Figure S1: Wind direction distributions: a) spring, b) summer, c) autumn, d) winter, e) unstable conditions and f) stable conditions. Unstable conditions were defined as h/Lmo<0 and stable conditions as h/Lmo>0, where Lmo is the Monin-Obukhov length and h is the measurement height.

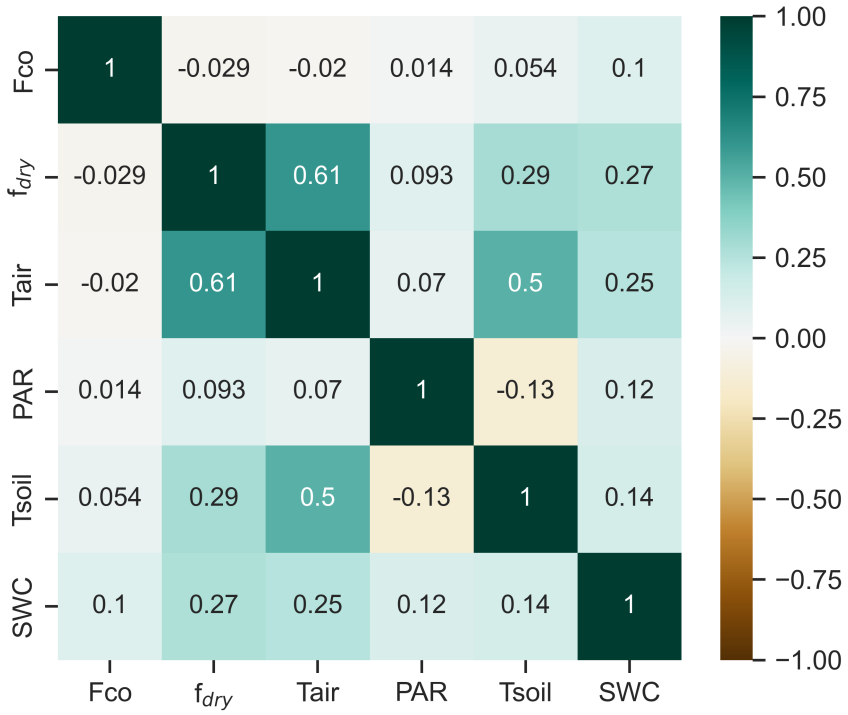

Figure S2: The correlation matrix of Spearman's rank correlation coefficients for wintertime CO flux (Fco) and flux drivers: soil temperature at a depth of 10 cm (Tsoil), soil water content at a depth of 10 cm (SWC), photosynthetically active radiation (PAR), air temperature (Tair), and fraction of dry surface area (f_{dry}) calculated for half-hourly values.

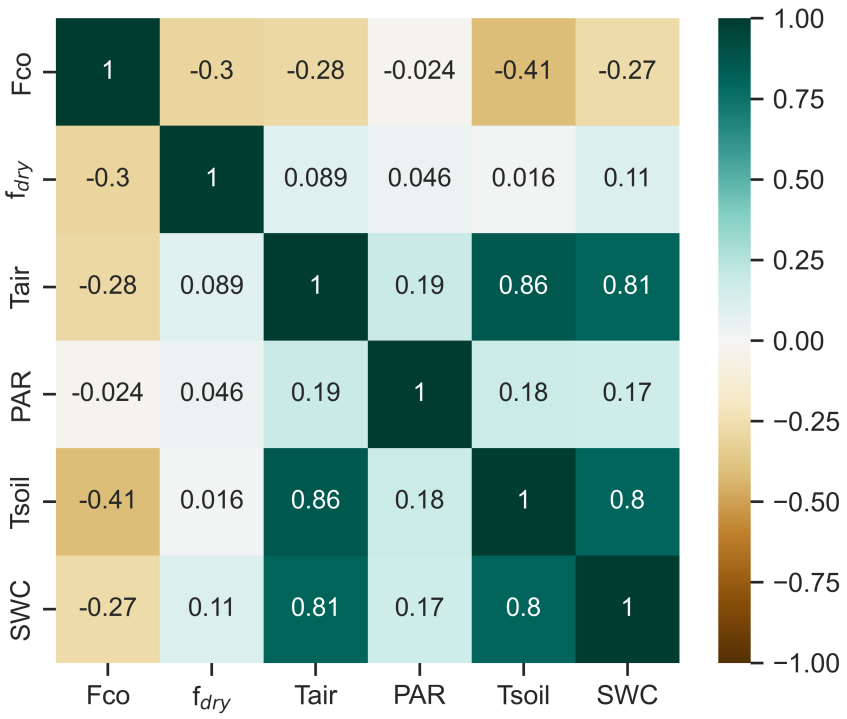

Figure S3: The correlation matrix of Spearman's rank correlation coefficients for nighttime CO flux (Fco) and flux drivers: soil temperature at a depth of 10 cm (Tsoil), soil water content at a depth of 10 cm (SWC), photosynthetically active radiation (PAR), air temperature (Tair), and fraction of dry surface area (f_{dry}) calculated for half-hourly values. Nighttime was defined as PAR <1 μmol m^{-2} s^{-1}.

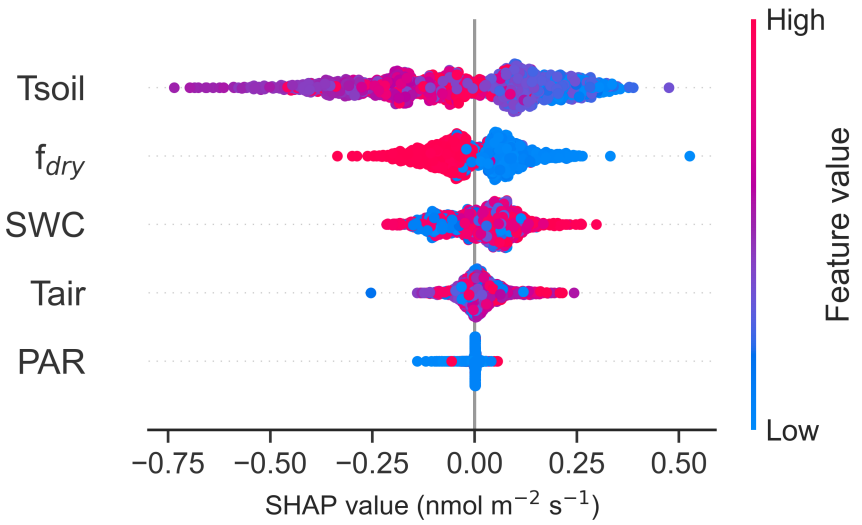

Figure S4: SHAP values of the nighttime RF model for CO flux drivers: photosynthetically active radiation (PAR), air temperature (Tair), soil temperature at a depth of 10 cm (Tsoil), soil water content at a depth of 10 cm (SWC) and fraction of dry surface area (f_{dry}). The SHAP values indicate the impact each feature has on the model output, with a negative value indicating a reduced flux and a positive value an increased flux. The blue color represents low feature values and red color high feature values. The zero line is the baseline (the average prediction). The SHAP values are calculated data from March to November and nighttime was defined as PAR < 1 µmol m^{-2}s^{-1}.

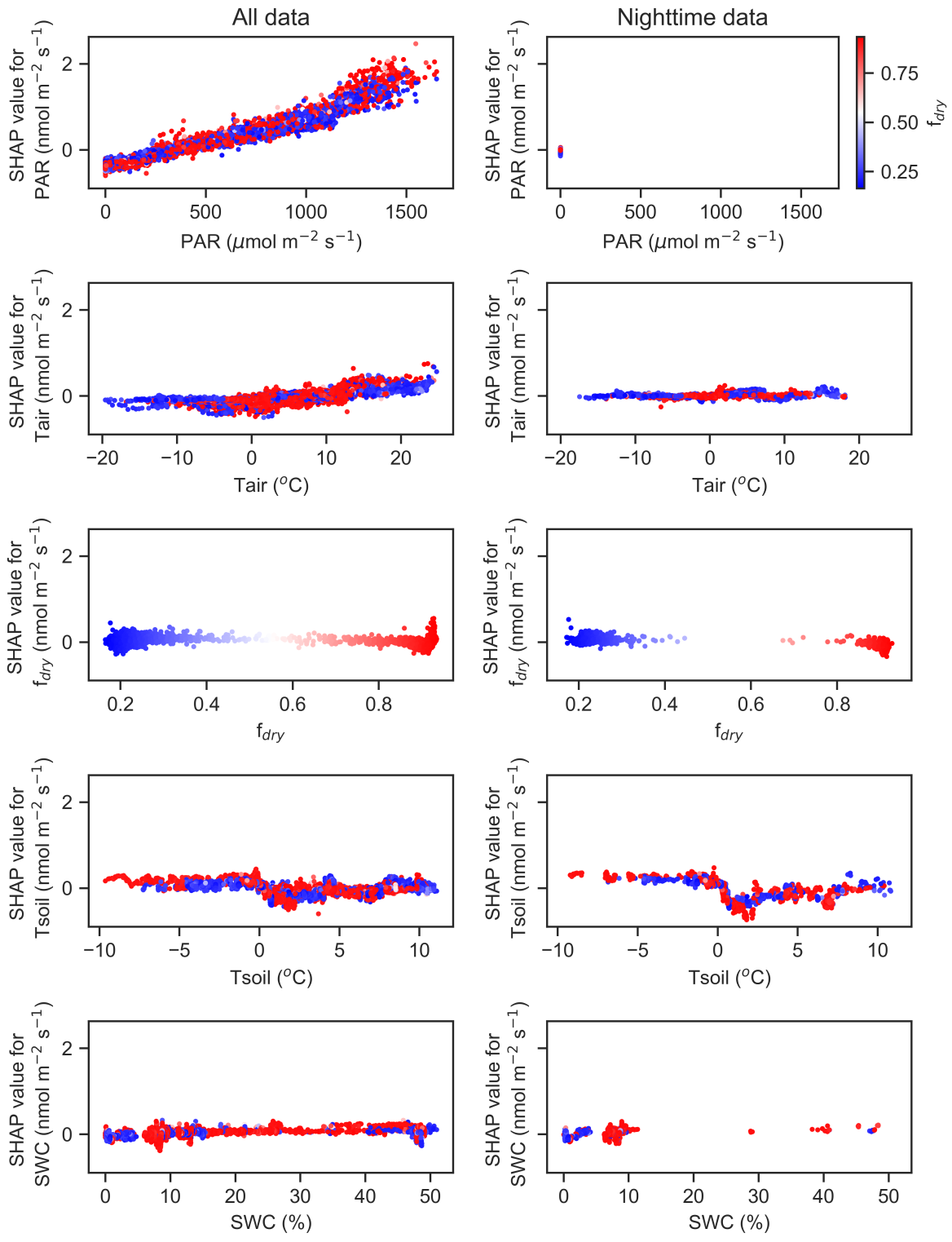

Figure S5: Partial dependence plots of SHAP values against features of RF model: photosynthetically active radiation (PAR), air temperature (Tair), soil temperature at a depth of 10 cm (Tsoil), soil water content at a depth of 10 cm (SWC), and fraction of dry surface area (f_{dry}). The colors represent interactions with surface cover type (f_{dry}), with red color indicating high f_{dry} and blue color indicating low f_{dry}. The left plots show relationships using all data, while the right plots are based on nighttime data.

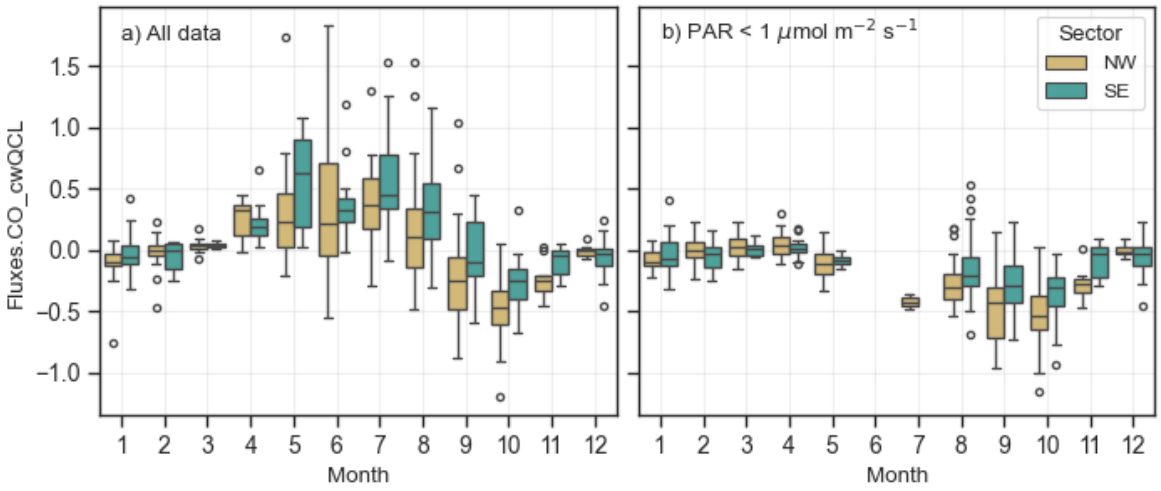

Figure S6: The boxplot of NW (yellow) and SE (turquoise) CO flux in different months a) all PAR levels and b) in dark conditions PAR <1 μmol m^{-2} s^{-1}. The box represents the interquartile range (IQR), with the lower limit at the 25th percentile and the upper limit at the 75th percentile, while the whiskers indicate the minimum and maximum values. Black dots represent outliers, defined as 1.5 $\times$ IQR.

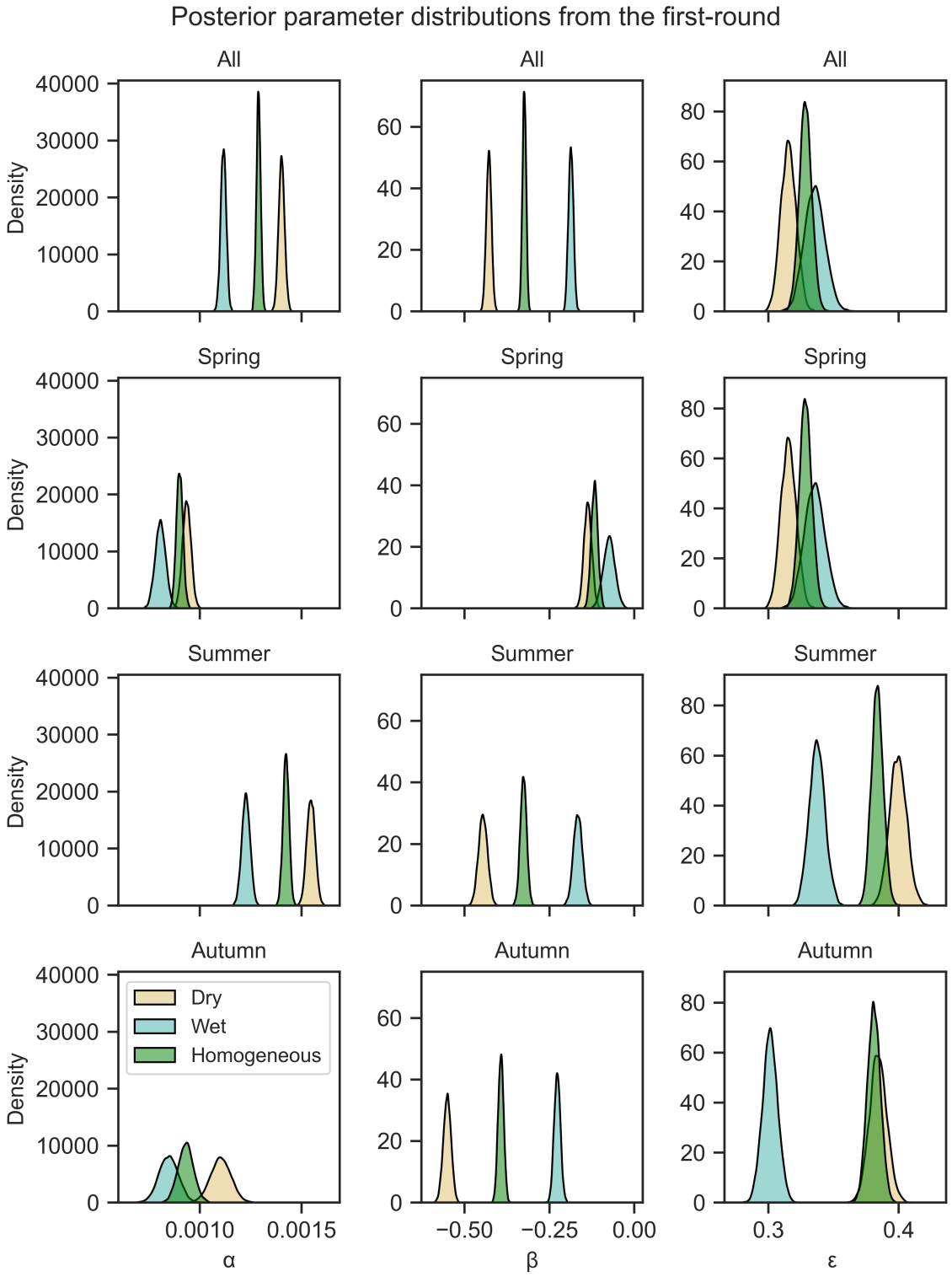

Figure S7: Posterior parameter distributions of the model parameters α, β, and residuals (ϵ) after the first model run. The parameters are estimated separatly for wet (turquoise) and dry (yellow). Homogeneous parameters represents the parameters without considering surface structure (green).

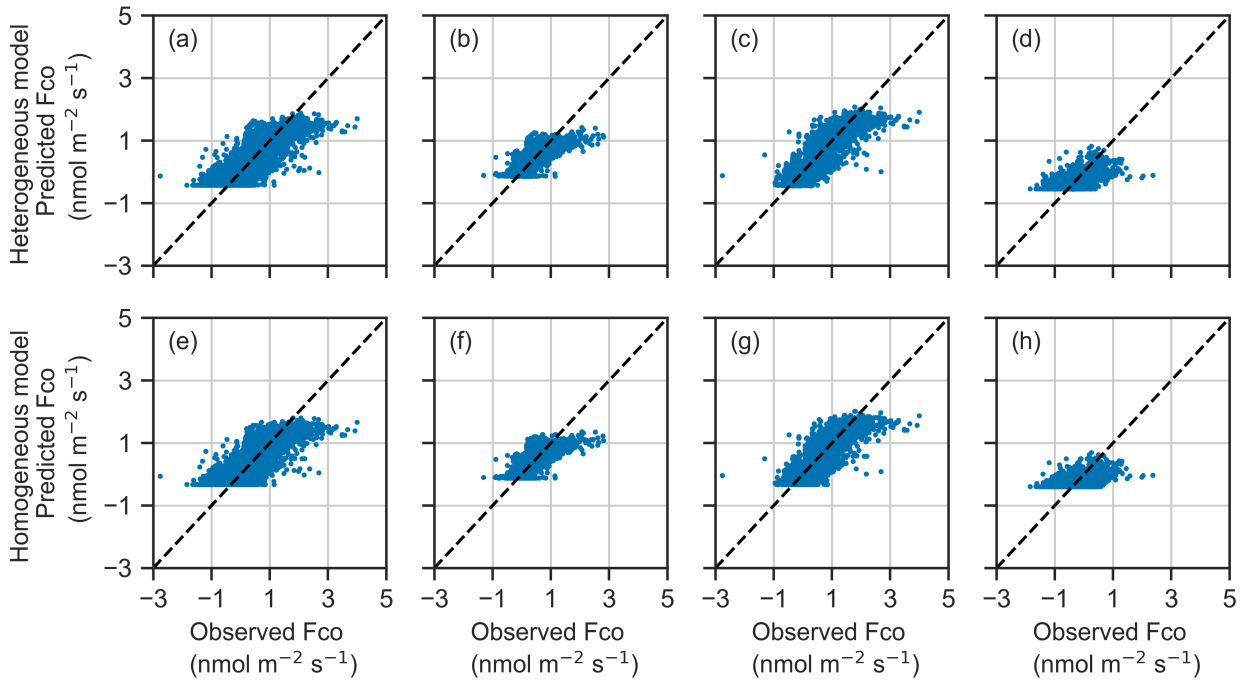

Figure S8: Predicted versus observed CO fluxes for: a) and e) all data, b) and f) spring, c) and g) summer, and d) and h) autumn. The top row shows fluxes from the heterogeneous model, while the bottom row shows fluxes from the homogeneous model. The black line represents the 1:1 relationship between observed and predicted values, and the blue dots represent 30-minute flux measurements.

Table S1: Priors distributions used in Bayesian inference approach.

Uniform distributions in first model run		
Parameter	Lower limit	Upper limit
α, α_{dry}, α_{wet}	0	1
β, β_{dry}, β_{wet}	-1	1
ϵ	0	1
Normal distributions in second model run (All data)		
Parameter	Mean	Standard deviation
α	0.00129	1.037e-5
β	-0.324	0.005
α_{dry}	0.00140	1.480e-5
β_{dry}	-0.428	0.008
α_{wet}	0.00112	1.357e-5
β_{wet}	-0.187	0.007
ϵ	0.4	0.004
Normal distributions in second model run (Spring)		
α	0.00090	1.600e-5
β	-0.118	0.010
α_{dry}	0.00094	2.084e-5
β_{dry}	-0.137	0.011
α_{wet}	0.00080	2.607e-5
β_{wet}	-0.074	0.017
ϵ	0.4	0.004
Normal distributions in second model run (Summer)		
Parameter	Mean	Standard deviation
α	0.00142	1.479e-5
β	-0.327	0.009
α_{dry}	0.00154	2.058e-5
β_{dry}	-0.446	0.013
α_{wet}	0.00123	2.028e-5
β_{wet}	-0.167	0.013
ϵ	0.4	0.004
Normal distributions in second model run (Autumn)		
Parameter	Mean	Standard deviation
α	0.00093	3.818e-5
β	-0.393	0.008
α_{dry}	0.00110	5.040e-5
β_{dry}	-0.551	0.011
α_{wet}	0.00084	4.776e-5
β_{wet}	-0.227	0.009
ϵ	0.4	0.004

Table S2: The model performance of the CO flux using posterior parameters from the second model run. Full indicates surface-type-specific model and simple is the linear model without considering surface structure.

Model	RMSE	R^2
Full (All)	0.378	0.658
Simple (All)	0.389	0.638
Full (Spring)	0.327	0.577
Simple (Spring)	0.328	0.574
Full (Summer)	0.372	0.736
Simple (Summer)	0.383	0.720
Full (Autumn)	0.350	0.296
Simple (Autumn)	0.380	0.169

Table S3: Annual cumulative CO fluxes for wet, dry and homogeneous surfaces, presented as mean, standard deviation (std), 25th percentile (Q25), and 75th percentile (Q75) confidence intervals.

Year	Stat	Dry	Wet	Homogeneous
2022–2023	Q25	-46.4	89.5	10.0
	Mean ± std	-44.0 ± 3.6	92.7 ± 4.7	11.6± 2.5
	Q75	-41.6	95.9	13.4
2023–2024	Q25	-53.8	81.3	2.5
	Mean ± std	-51.5 ± 3.5	84.4 ± 4.7	4.2± 2.4
	Q75	-49.1	87.5	5.8